

Thermodynamics of tetraphenylantimony acetophenoneoxymate

I. A. Letyanina · N. N. Smirnova · A. V. Markin ·
V. A. Ruchenin · V. N. Larina · V. V. Sharutin ·
O. V. Molokova

Received: 21 October 2009 / Accepted: 13 January 2010 / Published online: 8 January 2011
© Akadémiai Kiadó, Budapest, Hungary 2011

Abstract In the present research for the first time, the heat capacity C_p° of crystalline tetraphenylantimony acetophenoneoxymate $\text{Ph}_4\text{SbONCPhMe}$ has been measured using the methods of precision adiabatic vacuum calorimetry over the range from 6 to 350 K, the standard thermodynamic functions: heat capacity $C_p^\circ(T)$, enthalpy $H^\circ(T) - H^\circ(0)$, entropy $S^\circ(T)$, and Gibbs function $G^\circ(T) - H^\circ(0)$ have been calculated over the range from $T \rightarrow 0$ K to 350 K. Low-temperature ($20 \text{ K} \leq T \leq 50 \text{ K}$) heat capacity data have shown a chain-layered structure topology of the compound under study. The energy of combustion of the compound has been determined in the isothermal combustion calorimeter with a stationary bomb. The standard thermodynamic functions of formation of crystalline $\text{Ph}_4\text{SbONCPhMe}$ at 298.15 K have been calculated. The differential scanning calorimetry and thermogravimetric analysis studies have shown the compound melts with decomposition and its melting temperature has been estimated. Thermodynamic properties of $\text{Ph}_4\text{SbONCPhMe}$, Ph_5Sb and $\text{Ph}_4\text{SbONCPh}_2$ have been compared.

Keywords Tetraphenylantimony acetophenoneoxymate · Adiabatic vacuum calorimetry · Differential scanning calorimetry · Thermogravimetric analysis · Combustion calorimetry · Heat capacity · Thermodynamic functions · Standard thermodynamic functions

Introduction

Now it is known a huge number of organic derivatives of metals with different properties.

In recent years, the chemistry of organoantimony (V) complexes has attracted considerable attention due to the striking structure possibilities ranging from discrete monomeric structures to supramolecular assemblies [1–3]. It has been shown that the coordination number of the central atom in some antimony compounds can be equal to 6, 7, and 9.

In addition, organoantimony derivatives also exhibit significant antimicrobial properties as well as antitumor activities. The biological toxicity, however, is much less than that of Pt and Pd anticancer substances.

Synthesis and investigation of structures and physicochemical properties of organometallic compounds [4–6], particularly highly coordinated antimony compounds, are an actual task. The authors of [7, 8] have synthesized and investigated the structures and compositions of some individual organic compounds of antimony (V), for example, $\text{Ph}_4\text{SbONCPh}_2$, $\text{Ph}_3\text{Sb}(\text{ONCPh}_2)_2$, $\text{Ph}_4\text{SbONCHC}_4\text{H}_3\text{O}$, $\text{Ph}_4\text{SbONCPhMe}$, and others. Physicochemical characteristics of this group of compounds, particularly key thermodynamic quantities, are necessary as fundamental data and for calculating the thermal processes with these compounds' participation. Nowadays, thermodynamic characteristics of antimony (V) compounds are practically absent [9]. In Refs.

I. A. Letyanina · N. N. Smirnova (✉) · A. V. Markin ·
V. A. Ruchenin · V. N. Larina
Research Institute of Chemistry of Nizhny Novgorod State
University, Russian Federation, Prospekt Gagarina, 23/5,
Nizhny Novgorod, Russia 603950
e-mail: smirnova@ichem.unn.ru

V. V. Sharutin · O. V. Molokova
Blagoveschensk State Pedagogical University, Russian
Federation, ulitsa Lenina, 104, Blagoveschensk, Russia 675000

O. V. Molokova
Far Eastern Military Institute, Russian Federation,
ulitsa Lenina, 158, Blagoveschensk, Russia 675021

[10, 11], the energies of combustion of Me_3Sb and Ph_3Sb have been determined, and some thermodynamic quantities are given there. Earlier we have studied standard thermodynamic properties of Ph_5Sb [12] and $\text{Ph}_4\text{SbONCPh}_2$ [13] over the range from $T \rightarrow 0$ K to 450 K.

This study is a part of complex investigations of thermodynamic properties of antimony (V) compounds and describes the calorimetric investigation of heat capacity of tetraphenylantimony acetophenoneoxymate $\text{Ph}_4\text{SbONCPhMe}$ in the range from 6 to 350 K, calculation of standard ($p^\circ = 0.1$ MPa) thermodynamic functions: $C_p^\circ(T)$, $H^\circ(T) - H^\circ(0)$, $S^\circ(T)$, and $G^\circ(T) - H^\circ(0)$ of crystalline $\text{Ph}_4\text{SbONCPhMe}$ from $T \rightarrow 0$ K to 350 K using the experimental data, determination of combustion energy of the compound at $T = 298.15$ K, calculation of standard thermodynamic functions of formation of the compound at the same temperature, determination of fractal dimension D and estimation of structure topology and studying the melting of the compound using differential scanning calorimetry and thermogravimetric analysis.

Experimental

Sample

Tetraphenylantimony acetophenoneoxymate $\text{Ph}_4\text{SbONCPhMe}$ (gross formula $\text{C}_{32}\text{H}_{28}\text{SbO}_1\text{N}_1$) (**I**) was prepared in the Chemistry Department in Blagoveschensk State Pedagogical University according to the method described elsewhere [14]. A mixture of 1.00 g (1.97 mmol) of Ph_5Sb and 0.27 g (1.97 mmol) of $\text{HON}=\text{CMePh}$ in 10 ml of toluene was heated at 363 K for 1 h. After cooling, the solvent was removed and the residue was recrystallized from a toluene–heptane mixture (1:3). The yield was 1.05 g (94%). The compound **I** is stable in air and looks like light grey crystals.

X-ray diffraction analysis of the natural-faceted single crystals of **I** was carried out on a Bruker SMART-1000 CCD diffractometer. For compound **I**, the data were collected in sets of 606 frames at $\varphi = 0^\circ, 90^\circ, 180^\circ$, and 270° . Correction for absorption of X-rays by the samples was applied using face indices.

The structure of compound **I** was solved by the direct methods and refined by the least-squares method in anisotropic approximation for non-hydrogen atoms. Positions of hydrogen atoms were calculated geometrically and refined in the rider model.

Data collection and processing and refinement of the unit cell parameters were performed using the SMART and SAINT *Plus* programs [15]. Structure of **I** was solved and refined using the SHELXTL/PC programs [16].

Apparatus and measurement procedure

Heat capacity of **I** was measured over the range 6–350 K in a BKT-3.0 fully automatic adiabatic vacuum calorimeter with liquid helium and nitrogen used as cooling agents. The calorimeter design and measurement procedure are similar to those reported elsewhere [17, 18]. The reliability of this operation was tested by measuring the heat capacity of special purity copper, standard synthetic corundum and K-3 benzoic acid prepared at the D.I. Mendeleev All-Russian Institute for Metrology (VNIIM). It was established by the calibration that the determination of the heat capacity C_p° of substances was measured with an error not exceeding $\pm 2\%$ at $T = (6$ to $15)$ K, $\pm 0.5\%$ between 15 and 40 K, and $\pm 0.2\%$ in the range from 40 to 350 K. The phase transition temperatures are measured within about ± 0.01 K and the enthalpies of transformations with the error of $\pm 0.2\%$.

The heat capacity of **I** was measured between 6 and 350 K with a sample mass of 0.7005 g. The pressure of the heat-exchange gas (high-purity helium) in the calorimeter was 40 kPa at room temperature. In the BKT-3.0 calorimeter, 170 experimental C_p° values were obtained in two series of experiments. In the whole temperature range under study the heat capacity of **I** was 35–70% of the total heat capacity of the calorimetric ampoule with the substance. The experimental C_p° values were smoothed by the fitting to exponential and semi-logarithmic polynomials. The mean-square deviation of the C_p° points from the smooth curve did not exceed $\pm 0.9\%$ in the range 6–20 K, $\pm 0.2\%$ between 20 and 350 K.

The energy of combustion of **I** was measured in a modified isothermal combustion calorimeter B-08-MA with a stationary bomb [19]. Oxygen pressure in the bomb was 25×10^5 Pa. The energy equivalent of calorimeter ($W = 14805.1 \pm 2.5$ J Om^{-1}) was determined by the combustion of reference benzoic acid (mark K-3) (the double root of mean square derivation is given). The reliability of the calorimeter operation was checked by carrying out the combustion of reference succinic acid. The energy of combustion of this compound conformed to its passport value with the error of $\pm 0.017\%$.

The compound under investigation was combusted in melted paraffin in a thin-walled quartz crucible. The energy of combustion of paraffin was evaluated after several experiments: $\Delta_c U = -46744 \pm 8$ J g^{-1} . Paraffin was used as adjunct, and it ensured necessary temperature rising on the one hand, and it created favorable conditions for total oxidation of initial products on the other hand.

Thermal behavior of **I** in the range from 300 to 420 K was investigated with the differential scanning calorimeter DSC204F1 [20, 21], Germany, Netzsch Gerätebau. The

calorimeter was calibrated and tested against melting of *n*-heptane, mercury, tin, lead, bismuth, and zinc, with an error of ± 0.2 K in temperature and $\pm 1\%$ in the enthalpy of transition. The heating rate was 5 K min^{-1} , the measurement was carried out in argon atmosphere. It was put 0.027 g of the compound under study to the crucible.

Thermogravimetric analysis of **I** was done using thermal microbalance TG209F1, Germany, Netzsch Gerätebau. TG-analysis was carried out in the range from 300 to 470 K in the argon atmosphere. The thermal microbalance TG209F1 allows fixing the mass change in ± 0.1 mcg. The mean heating rate was 5 K min^{-1} . The measuring technique of the TG-analysis was standard, according to Netzsch Software Proteus.

Results and discussion

Heat capacity

Experimental values of heat capacity of **I** over the range from 6.21 to 352.51 K (Table 1) and the smoothed $C_p^\circ = f(T)$ plot are illustrated in Fig. 1. In the temperature range under study, the heat capacity of **I** rises gradually with temperature increasing without anomaly. The dependence is similar to one for pentaphenylantimony Ph_5Sb [12] and tetraphenylantimony benzophenoneoxymate $\text{Ph}_4\text{SbONCPh}_2$ [13], which we have studied earlier (Fig. 1). The values of heat capacity of Ph_5Sb at $T > 30$ K are greater than the values for oxymates ($\sim 12\%$ in the case of **I** and $\sim 20\%$ in the case of $\text{Ph}_4\text{SbONCPh}_2$). This can be explained by the replacement of one of phenylic radicals in Ph_5Sb by a more difficult oxymate group. At $T < 50$ K, the differences in heat capacities of the compounds under study do not exceed 10%. This is connected with the similarity of their structures. As it is known [22], at $T < 50$ K a contribution into total heat capacity is made by lattice vibrations, group vibrations are excited at $T > 50$ K and that leads to the rising of the difference in the heat capacity values of the compounds under study.

Low-temperature heat capacity data were used to calculate a value of a fractal dimension D [23]. The fractal dimension is an exponent at temperature in the basic equation in the fractal version of Debye's theory of heat capacity of solids. The value of D gives a possibility to draw a conclusion about a character of a topology structure of a compound. D can be obtained from a $\ln C_v - \ln T$ plot for a compound [23]. It follows from Eq. 1:

$$C_v = 3D(D+1)kN\gamma(D+1)\zeta(D+1)(T/\theta_{\max})^D. \quad (1)$$

Here N is the number of atoms in a molecular unit, k is the Boltzmann constant, $\gamma(D+1)$ is the γ -function, $\zeta(D+1)$ is

Table 1 Experimental data of molar heat capacity of tetraphenylantimony acetophenoneoxymate in $\text{J mol}^{-1} \text{K}^{-1}$; $M = 564.33 \text{ g mol}^{-1}$, $p^\circ = 0.1 \text{ MPa}$

T/K	C_p°
<i>Series 1</i>	
6.21	3.39
6.31	3.56
6.43	3.75
6.53	3.91
6.62	4.07
6.72	4.25
6.82	4.42
6.93	4.61
7.03	4.81
7.14	5.01
7.24	5.21
7.35	5.42
7.45	5.63
7.55	5.84
7.66	6.06
7.77	6.29
7.89	6.53
8	6.77
8.12	7.02
8.23	7.25
8.35	7.49
8.46	7.73
8.57	7.96
8.68	8.19
8.8	8.42
8.91	8.66
9.02	8.91
9.14	9.17
9.26	9.45
9.38	9.78
9.49	10
9.62	10.3
9.73	10.5
9.84	10.8
9.98	11.2
10.34	12
10.72	13.2
11.19	14.5
11.66	15.8
12.14	16.9
12.63	18.7
13.13	20.1
13.65	21.5
14.16	23
14.68	24.5

Table 1 continued

T/K	C_p^o
15.21	26.31
15.74	27.87
16.28	29.18
16.82	31.06
17.36	33.07
17.95	34.99
18.5	36.91
19.06	38.62
19.62	40.65
20.18	42.91
21.37	46.84
22.97	52.22
24.58	57.52
26.22	62.99
27.86	68.74
29.51	74.68
31.17	80.56
32.84	86.23
34.52	91.76
36.21	97.51
37.9	102.7
39.6	108.1
41.3	113.3
43.01	118.6
44.72	123.9
46.44	129.1
48.2	134.5
49.92	139.7
51.64	144.6
53.8	151
56.33	157.5
58.07	162
59.81	166.2
61.8	171.1
63.8	175.6
65.69	180.2
67.29	184
69.03	188
70.78	192.2
72.6	196.5
74.7	201
77.01	205.6
79.14	210
81.25	214.1
83.35	217.7
85.44	221.2
87.52	225.2

Table 1 continued

T/K	C_p^o
<i>Series 2</i>	
83.67	220
87.35	225.2
90.91	230.8
94.46	236.1
98.01	241.7
101.56	247
105.11	252.8
108.65	258.6
112.2	264.7
115.75	270.7
119.3	276.5
123.12	283.5
126.85	289.2
130.41	294.6
133.96	300.3
137.51	306.1
141.06	311.6
144.62	316.6
148.27	322.8
151.92	328.1
155.82	334.9
159.5	340.8
163.3	347.7
166.86	353.3
170.81	360.3
174.76	367.2
178.48	373.5
182.21	379.5
186.7	387.5
190.83	394.3
194.39	400.9
197.95	406.1
201.52	412.2
205.09	418.8
208.66	424.6
212.23	431.2
215.8	438.1
219.35	444.8
222.91	451
226.45	457.1
230.05	463.6
233.64	471
237.25	476.6
240.78	484
244.3	489.9
247.82	496.5

Table 1 continued

T/K	C_p°
251.34	503.3
254.85	509.8
256.54	512.9
260.09	519.3
263.58	527.2
267.17	533.9
270.68	540.4
274.15	547.7
277.61	554.6
281.05	561.5
284.49	568.5
287.37	573.6
290.79	580.2
294.19	586.8
297.59	594
300.95	601.1
303.98	607.8
307.01	614
310.33	621.3
313.66	627.5
316.97	634
320.3	641.8
323.54	648.3
326.81	654.7
330.06	662.1
333.3	668.1
336.52	675
339.7	682.6
342.88	689.3
346.04	695.2
349.16	701.8
352.51	709.4

the Riemann ξ -function, and θ_{\max} is the characteristic temperature. For a particular solid, $3D(D+1)kN\gamma(D+1)\xi(D+1)(1/\theta_{\max})^D = A$ is a constant value and Eq. 1 can be written as Eq. 2:

$$\ln C_v = \ln A + D \ln T. \quad (2)$$

At $T < 50$ K, the experimental values of C_p° are equal to C_v . Thus, using experimental heat capacity data in the range from 20 to 50 K and Eq. 2, the value of the fractal dimension can be obtained. D for **I** is equal to 1.5, the characteristic temperature $\theta_{\max} = 218.7$ K. At calculated values of D and θ_{\max} , Eq. 1 reproduces the C_p° values over this temperature range with an error in $\pm 0.3\%$.

According to the multifractal version of the theory of heat capacity of solids [24], $D = 1$ corresponds to the

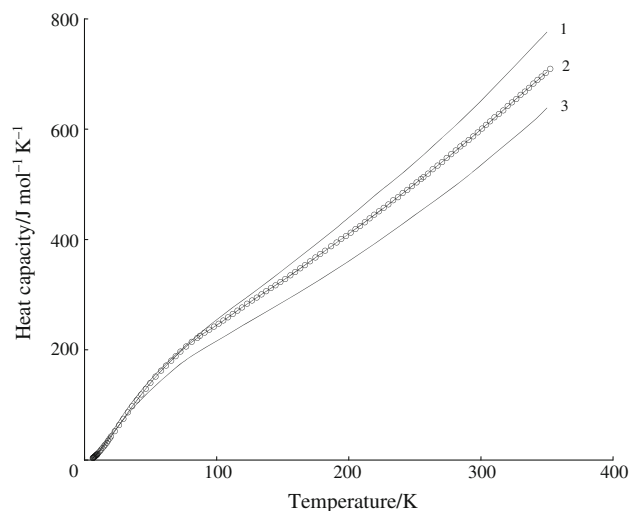


Fig. 1 Heat capacity of $\text{Ph}_4\text{SbONCPh}_2$ [13] (curve 1), $\text{Ph}_4\text{SbONCPhMe}$ (curve 2) and Ph_5Sb [12] (curve 3)

Table 2 Fractal dimensions D and characteristic temperatures θ_{\max}

Compound	Temperature range/K	D	θ_{\max}/K	$\delta^a/\%$
Ph_5Sb^b	20–50	1.3	246.7	1.0
$\text{Ph}_4\text{SbONCPh}_2^c$	20–50	1.5	202.8	0.5
$\text{Ph}_4\text{SbONCPhMe}$	20–50	1.5	218.7	1.0

Number of degrees of freedom $n = 28$

^a Error in the fitting

^b Values of D and θ_{\max} have been calculated using data from [12]

^c Values of D and θ_{\max} have been taking from [13]

solids with a chain structure, $D = 2$ corresponds to ones with a layered structure, and $D = 3$ corresponds to ones with a spatial structure. Obtained value of D points out the chain-layer topology structure of **I**. The results of low-temperature heat capacity data processing for **I** and for studied earlier Ph_5Sb [12] and $\text{Ph}_4\text{SbONCPh}_2$ [13] are presented in Table 2. Values of the characteristic temperatures θ_{\max} calculated for the same number of degrees of freedom and temperature range allow us to make the inference about relative hardness of the structures of solids. According to the results, $\theta_{\max}(\text{Ph}_5\text{Sb}) > \theta_{\max}(\text{Ph}_4\text{SbONCPhMe}) > \theta_{\max}(\text{Ph}_4\text{SbONCPh}_2)$. Thus, the hardness of crystalline structures of the compared compounds changes in the same row. Evidently, this tendency remains at higher temperatures too.

Standard thermodynamic functions

To calculate the standard thermodynamic functions (Table 3) of **I**, its C_p° values were extrapolated from 6 K to

Table 3 Standard thermodynamic functions of tetraphenylantimony tetraphenoneoxymate; $M = 564.33 \text{ g mol}^{-1}$

T/K	$C_p^\circ/\text{J mol}^{-1} \text{ K}^{-1}$	$H^\circ(T) - H^\circ(0)/\text{kJ mol}^{-1}$	$S^\circ(T)/\text{J mol}^{-1} \text{ K}^{-1}$	$-[G^\circ(T) - H^\circ(0)]/\text{kJ mol}^{-1}$
5	1.80	0.00230	0.602	0.000753
10	11.2	0.0321	4.37	0.0115
15	25.5	0.123	11.6	0.0502
20	42.11	0.2911	21.10	0.1310
25	58.91	0.5441	32.32	0.2640
30	76.38	0.8818	44.59	0.4559
40	109.3	1.814	71.19	1.033
50	139.9	3.061	98.89	1.883
60	166.7	4.599	126.9	3.012
70	190.3	6.385	154.3	4.418
80	211.7	8.399	181.2	6.097
90	229.5	10.61	207.2	8.039
100	244.5	12.97	232.1	10.24
120	277.9	18.20	279.6	15.36
140	309.7	24.08	324.9	21.41
160	341.8	30.59	368.3	28.34
180	376.1	37.76	410.5	36.13
200	409.8	45.62	451.9	44.76
220	445.7	54.18	492.6	54.20
240	481.9	63.45	533.0	64.46
260	520.0	73.47	573.0	75.52
280	559.0	84.26	613.0	87.38
298.15	595.4	94.73	649.2	98.83
300	599.2	95.83	652.9	100.0
310	620.0	101.9	672.9	106.7
320	641.0	108.2	692.9	113.5
330	661.8	114.7	713.0	120.5
340	682.5	121.5	733.0	127.8
350	703.9	128.4	753.1	135.2

zero temperature according to the Debye law in the low-temperature limit [9]:

$$C_p^\circ = nD(\theta_D/T), \quad (3)$$

where n is the number of degrees of freedom, D denotes Debye function, θ_D is Debye characteristic temperature. $n = 6$ and $\theta_D = 64.55 \text{ K}$ are specially selected parameters. Equation 3 with these parameters describes the experimental C_p° values of the compound between $T = 6 \text{ K}$ and $T = 11 \text{ K}$ with the error of $\pm 0.9\%$. In calculating the functions, it was assumed that Eq. 3 reproduced C_p° values of **I** at $T < 6 \text{ K}$ with the same error.

The calculation of enthalpy and entropy was made by the numerical integration of $C_p^\circ = f(T)$ and $C_p^\circ = \ln f(T)$ curves, respectively. The Gibbs function was calculated with Gibbs–Helmholtz equation from the enthalpies and entropies at the corresponding temperatures [25]. It was

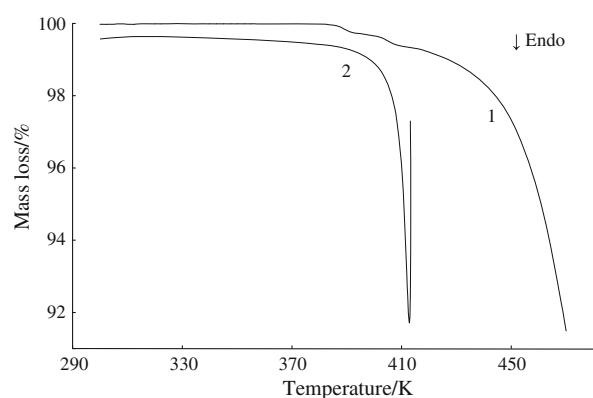


Fig. 2 Plot of the TG-signal (curve 1) and DSC-signal (curve 2) against temperature for $\text{Ph}_4\text{SbONCPhMe}$

suggested that the error of the function values was $\pm 2\%$ at $T < 15 \text{ K}$, $\pm 0.5\%$ between 15 and 40 K, $\pm 0.2\%$ in the range from 40 to 350 K.

Table 4 Data on Ph₄SbONCPhMe combustion experiments

<i>m</i>	<i>Q</i>	<i>q</i> (par)	<i>q</i> (th)	<i>q</i> (HNO ₃)	<i>q</i> (Sb ₂ O ₃)	<i>q</i> (C + Sb)	−Δ _c <i>U</i>
0.19844	39243.4	32980.0	37.0	18.8	5.5	62.7	17847.5
0.20372	39583.5	33183.3	40.0	9.4	5.6	79.7	17828.6
0.19820	39374.6	33131.0	34.6	17.9	5.5	50.9	17788.3
0.20330	39654.3	33242.7	36.8	19.9	5.6	49.2	17789.7
0.20126	39615.4	33279.1	35.8	17.0	5.6	76.9	17850.4
0.20333	27043.3	33206.7	41.5	9.4	5.6	79.4	17826.0

Note: Δ_c*U* is the energy of combustion of samples under calorimetric bomb conditions/kJ mol^{−1} (mean value: Δ_c*U*(Ph₄SbONCPhMe) = −17822 ± 22 kJ mol^{−1}) *m* is the weight of the sample subjected to combustion/g, *Q* is the total amount of released energy/J, *q*(par), *q*(th), *q*(HNO₃), *q*(Sb₂O₃) and *q*(C + Sb) are the corrections for the energies of combustion of paraffin and cotton thread and the energies of formation of aqueous HNO₃, crystalline Sb₂O₃, amorphous carbon and metallic antimony, respectively/J, Δ_c*U* is the energy of combustion of samples under calorimetric bomb conditions (mean value: Δ_c*U*(Ph₄SbONCPhMe) = −17822 ± 22 kJ mol^{−1})

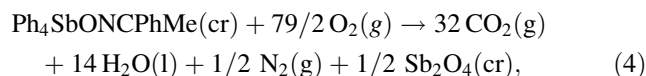
Melting

The melting of **I** was studied in two independent experiments using methods of differential scanning calorimetry and thermogravimetric analysis. Corresponding curves are presented in Fig. 2. As can be seen that evident mass loss (*m*/*m*₀) begins from 390 K, at *T* = 420 K, *m*/*m*₀ = 0.7%, at *T* = 450 K, *m*/*m*₀ = 8%. Consequently, from *T* = 390 K, the sample of compound **I** is thermally unstable and decomposes. These findings (Fig. 2, curve 1) compare favorably to those reported in DSC-analysis (Fig. 2, curve 2). From the temperature measurement begins at *T* = 300 K, the DSC-signal is a straight line that points out the thermal stability of the compound. Then from *T* = 390 K, an endothermic effect is seen, which does not finish. This is conditioned by the melting of the sample of **I**, accompanied by partial compound decomposition. The estimated value of melting temperature was taken by us as the temperature corresponding to the minimum of the DSC-curve [25]. Thus, *T*_{fus}^o = (417.6 ± 0.3) K.

Enthalpy of combustion and standard thermodynamic characteristics of formation of Ph₄SbONCPhMe at *T* = 298.15 K

The energy of combustion of crystalline Ph₄SbONCPhMe was measured in six experiments. The sample mass was approximately 0.2 g. The experimental data are listed in Table 4. After the experiments, the analysis of combustion products was made. Some trace dark spots were revealed visually on the crucible walls and indicated carbon formation. According to X-ray diffraction data, the solid combustion products contained antimony tetraoxide Sb₂O₄, trioxide Sb₂O₃, and free antimony. Qualitative and quantitative composition of solid products of **I** combustion corresponded to the compositions, which were determined after the combustion of

Me₃Sb [10] and Ph₃Sb [11] in the same conditions, and the combustion of Ph₅Sb and Ph₄SbONCPh₂ made by us [12, 13]. Corrections for partial oxidation of metal were made (Table 4). In the Δ*U*_c calculation, usual corrections were adopted. They were for the combustion of a cotton thread used for sample firing, for the combustion of paraffin used in the experiment, for HNO₃ solution formation. We used the following equation to describe the combustion process:



where cr is crystal, g is gas, l is liquid.

As there were both Sb₂O₄ and Sb₂O₃ in the solid combustion products, in the calculation of the enthalpy of combustion, a correction for partial oxidation of the investigated compound was adopted [26]. In addition, the Washburn correction ($\pi = -0.0395\%$) and the correction for the change in the number of moles of gaseous reagents ($\Delta n = -7.5$ mol) were taken into account. The resulting standard enthalpy of combustion of tetraphenylantimony acetophenoneoxymate at *T* = 298.15 K was Δ_c*H*^o(298.15, Ph₄SbONCPhMe, cr) = −17832.0 ± 22.7 kJ mol^{−1}.

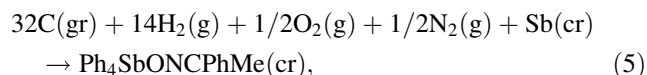
The standard enthalpy of combustion of Ph₄SbONCPhMe and the literature data on the standard enthalpies of formation of gaseous CO₂ [27], liquid water [27], and crystalline Sb₂O₄ [28] were used to calculate the standard enthalpy of formation of crystalline Ph₄SbONCPhMe at *T* = 298.15 K. It was Δ_f*H*^o(298.15, Ph₄SbONCPhMe, cr) = 801.0 ± 28.8 kJ mol^{−1}.

Using the value of the absolute entropy of **I** (Table 3) and the simple substances—carbon [29], hydrogen [27], oxygen [27], nitrogen [27], and antimony [30], the standard entropy of formation of **I** at *T* = 298.15 K was estimated. It was Δ_f*S*^o(298.15, Ph₄SbONCPhMe, cr) = −1607.9 ± 2.1 J mol^{−1} K^{−1}.

The standard Gibbs function of formation of **I** at the same temperature was calculated from the standard enthalpy and

entropy values by the Gibbs–Helmholtz equation. It was $\Delta_f G^\circ(298.15, \text{Ph}_4\text{SbONCPhMe, cr}) = 1280.4 \pm 28.8 \text{ kJ mol}^{-1}$.

Obtained values fit the equation:



where gr is graphite.

Conclusions

- The heat capacity of crystalline tetraphenylantimony acetophenoneoximate has been measured over the range from 6 to 350 K.
- Using low-temperature heat capacity data, the structure topology of tetraphenylantimony acetophenoneoximate has been established as chain-layer one.
- It has been revealed that tetraphenylantimony acetophenoneoximate melts with a partial decomposition.
- From experimental data, the standard thermodynamic functions of tetraphenylantimony acetophenoneoximate, namely, the heat capacity $C_p^\circ(T)$, enthalpy $H^\circ(T) - H^\circ(0)$, entropy $S^\circ(T)$, and Gibbs function $G^\circ(T) - H^\circ(0)$ have been calculated over the range from $T \rightarrow 0$ to 350 K.
- The energy of combustion of crystalline tetraphenylantimony acetophenoneoximate at $T = 298.15 \text{ K}$ has been determined.
- The values of standard thermodynamic functions of formation of tetraphenylantimony acetophenoneoximate at $T = 298.15 \text{ K}$ have been calculated.

References

1. Molokova OV, Sharutin VV, Sharutina OK, Alyab'eva EA, Kuharev YuA. Oximates of tetra- and triarylantimony. Synthesis and structures. Chem Comput Simul Butlerov Commun. 2004;5:28–33.
2. Gupta A, Sharma RK, Bohra R, Jain VK, Drake JE, Hursthouse MB, Light ME. Synthetic, spectroscopic and structural aspects of triphenylantimony(V) complexes with internally functionalized oximes: crystal and molecular structure of $[\text{Ph}_3\text{Sb}\{\text{ON}=\text{C}(\text{Me})\text{C}_5\text{H}_4\text{N}-2\}]_2$. Polyhedron. 2002;21:2387–92.
3. Dodonov VA, Gushchin AV, Gor'kaev DA, Fukin GK, Starostina TI, Zakharov LN, Kurskii YuA, Shavyrin AS. Synthesis and structures of triphenylantimony oximates. Russ Chem Bull. 2002;51:1051–7.
4. Luan SR, Zhu YH, Jia YQ, Cao Q. Characterization and thermal analysis of thiourea and bismuth trichloride complex. J Therm Anal Calorim. 2010;99:523–530.
5. Fomin VM, Markin AV. Oxidation mechanism of ferrocene with molecular oxygen. Kinetic and thermodynamic aspects. J Therm Anal Calorim. 2008;92:985–7.
6. Ribeiro da Silva MAV, Santos AFLM. Energetics of some sulphur heterocycles. Thiophene derivatives. J Therm Anal Calorim. 2009;95:333–44.
7. Sharutin VV, Sharutina OK, Molokova OV, Ettenko EN, Krivolapov DB, Gubaidullin AT, Litvinov IA. Synthesis and structure of tetra- and triarylantimony oximates. Russ J Gen Chem. 2001;71:1243–7.
8. Sharutin VV, Sharutina OK, Molokova OV, Ettenko EN, Krivolapov DB, Gubaidullin AD, Litvinov IA. Synthesis and structure of tetra- and triarylantimony oximates. Russ J Gen Chem. 2002;72:893–8.
9. Rabinovich IB, Nistratov VP, Telnoy VI, Sheiman MS. Thermochemical and thermodynamic properties of organometallic compounds. New York: Begell House Inc. Publishers; 1999.
10. Long LH, Sackman JF. The heat of formation of antimony trimethyl. Trans Faraday Soc. 1955;51:1062–4.
11. Birr K-H. Bildungswärmen von Triphenylphosphin und Triphenylstibin. Zeitschrift für anorganische und allgemeine Chemie. 1960;306:21–4.
12. Smirnova NN, Letyanina IA, Larina VN, Markin AV, Sharutin VV, Senchurin VS. Thermodynamic properties of pentaphenylantimony Ph_5Sb over the range from $T \rightarrow 0 \text{ K}$ to 400 K. J Chem Thermodyn. 2009;41:46–50.
13. Smirnova NN, Letyanina IA, Markin AV, Larina VN, Sharutin VV, Molokova OV. Thermodynamic properties of tetraphenylantimony benzophenoximate in the region of 0–450 K. Russ J Gen Chem. 2009;79:717–23.
14. Sharutin VV, Sharutina OK, Molokova OV, Pakusina AP, Gerasimenko AV, Sergienko AS, Bukvetskii BV, Popov DYU. Synthesis and structures of tetra- and triarylantimony oximates. Russ J Coord Chem. 2002;28:544–55.
15. SMART and SAINT. Area detector control and integration software. Madison: Bruker AXS Inc.; 1998.
16. Sheldrick GM. SHELXTL/PC, versions 5.10: an integrated system for solving, refining and displaying crystal structures from diffraction data. Madison: Bruker AXS Inc.; 1998.
17. Varushchenko RM, Druzhinina AI, Sorkin EL. Low-temperature heat capacity of 1-bromoperfluorooctane. J Chem Thermodyn. 1997;29:623–7.
18. Malyshev VM, Milner GA, Sorkin EL, Shibakin VF. Automatic low-temperature calorimeter. Prib i Teh Eksp. 1985;6:195–7.
19. Kir'yanov KV, Telnoy VI. Using the calorimeter B-08 for precision measuring of a combustion heat. Tr po Him i Him Tehnol. 1975;4:10910.
20. Höhne GWH, Hemminger WF, Flammersheim H-J. Differential scanning calorimetry. 2nd ed. Heidelberg: Springer; 2003.
21. Drebuschak VA. Calibration coefficient of heat-flow DSC. Part II. Optimal calibration procedure. J Therm Anal Calorim. 2005;79:213–8.
22. Lebedev BV, Smirnova NN. Chemical thermodynamics of polyalkanes and polyalkenes. Nizhny Novgorod: NNSU Press; 1999.
23. Lazarev VB, Izotov AD, Gavrichev KS, Shebershneva OV. Fractal model of heat capacity for substances with diamond-like structures. Thermochim Acta. 1995;269–270:109–16.
24. Tarasov VV. Theory of heat capacity of chain and layer structures. J Fiz Him. 1950;24:111–28.
25. Smirnova NN, Lebedev BV, Bykova TA, Markin AV, Tur DR. Thermodynamic properties of poly[bis(trifluoroethoxy)phosphazene] in the range from $T \rightarrow 0$ to 620 K. J Therm Anal Calorim. 2009;95:229–34.
26. Telnoy VI, Kir'yanov KV, Ermolaev VI, Rabinovich IB. Thermochemistry of dicyclopentadienil compounds of transition elements of the 3-d row in the periodic system. Dokl Akad Nauk SSSR. 1975;220:1088–91.

27. Chase Jr MW. NIST-JANAF thermochemical tables (4th edition). J Phys Chem Ref Data Monogr. 1998;9:1951. Database <http://webbook.nist.gov/chemistry/>.
28. Simon A, Thaler E. Beiträge zur Kenntnis von Oxyden. Zur Kenntnis der Oxyde des Antimons. Zeitschrift für anorganische und allgemeine Chemie. 1927;162:253–78.
29. Cox JD, Wagman DD, Medvedev VA. Codata key values for thermodynamics. New York: Hemisphere Publishing Corp; 1984. Database <http://webbook.nist.gov/chemistry/>.
30. DeSorbo W. The low temperature specific heat of antimony. Acta Metall. 1953;1:503–7.